

# Reversibly Light-Modulated Dirac Point of Graphene Functionalized with Spiropyran

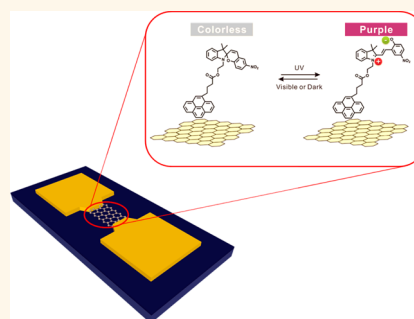
A-Rang Jang,<sup>†,\*,5</sup> Eun Kyung Jeon,<sup>†</sup> Dongwoo Kang,<sup>†</sup> Gwangwoo Kim,<sup>†</sup> Byeong-Su Kim,<sup>†,\*</sup> Dae Joon Kang,<sup>5,\*</sup> and Hyeon Suk Shin<sup>†,\*,\*</sup>

<sup>†</sup>Interdisciplinary School of Green Energy, Low Dimensional Carbon Materials Center, KIER-UNIST Advanced Center for Energy and <sup>‡</sup>Institute of Biological and Chemical Sciences, Ulsan National Institute of Science & Technology (UNIST), UNIST-gil 50, Ulsan 689-805, Korea and <sup>5</sup>BK21 Physics Research Division, Department of Energy Science, SKKU Advanced Institute of Nanotechnology, Sungkyunkwan University, Suwon 440-746, Korea

Graphene with perfect two-dimensional (2D) carbon crystalline structure is currently at the center of attention because of its high electrical/thermal conductivity, high mobility, high mechanical property, and quantum Hall effect.<sup>1,2</sup> In particular, graphene growth in large area and its transfer onto any substrate have attracted many researchers to become involved in its study for various applications, beyond the interests of the basic science fields.<sup>3–5</sup> Graphene has a unique electronic band structure, in that the conduction and valence bands meet at a single point, the Fermi level at the K point, which is called the Dirac point. This enables both electron and hole to transport. Because of such band structure, field-effect transistor (FET) devices with graphene have shown ambipolar properties.<sup>6–8</sup>

Tuning of the energy level and resulting control of the electronic properties of graphene, which is required for realization of electronic devices and related applications, have been explored by making nanoribbon and nanomesh structures of graphene, preparing bilayer graphene, and doping of graphene.<sup>9–17</sup> Among these approaches, doping of graphene is now considered to be the easiest way to control its electrical property. The doping can be classified into some categories according to the method for doping. For instance, substitutional doping is the most common method: replacing the carbon element in graphene with nitrogen under ammonia flow at high temperature induces n-type doping.<sup>15,16</sup> Substitutional doping usually has a drawback, such as a decrease in the mobility and conductivity of graphene, because substitutional doping introduces large amounts of defects into graphene.<sup>15–17</sup> This substitutional doping is a kind of functionalization of graphene by covalent bonding. In addition to such substitution, the introduction of functional groups into graphene by covalent bonding also changes

## ABSTRACT



Graphene has been functionalized with spiropyran (SP), a well-known photochromic molecule. It has been realized with pyrene-modified SP, which has been adsorbed on graphene by  $\pi-\pi$  interaction between pyrene and graphene. The field-effect transistor (FET) with SP-functionalized graphene exhibited n-doping effect and interesting optoelectronic behaviors. The Dirac point of graphene in the FET could be controlled by light modulation because spiropyran can be reversibly switched between two different conformations, a neutral form (colorless SP) and a charge-separated form (purple colored merocyanine, MC), on UV and visible light irradiation. The MC form is produced during UV light irradiation, inducing the shift of the Dirac point of graphene toward negative gate voltage. The reverse process back to the neutral SP form occurred under visible light irradiation or in darkness, inducing a shift of the Dirac point toward positive gate voltage. The change of the Dirac point by UV and visible light was reproducibly repeated. SP molecules also improved the conductance change in the FET device. Furthermore, dynamics on conversion from MC to SP on graphene was different from that in solution and solid samples with SP-grafted polymer or that on gold nanoparticles.

**KEYWORDS:** graphene · spiropyran · doping · photochromic molecule

its electrical properties.<sup>18–20</sup> However, graphene functionalized by covalent bonding has similar drawbacks to the common doping technique because of defects generation, inducing a decrease in mobility and the on/off ratio in a graphene FET. On the other hand, functionalization of graphene by non-covalent bonding does not basically generate defects. This method is expected to be one of the solutions to solve the problems of common doping processes. Actually,

\* Address correspondence to  
shin@unist.ac.kr,  
djikang@skku.edu,  
bskim19@unist.ac.kr.

Received for review August 6, 2012  
and accepted September 13, 2012.

Published online September 13, 2012  
10.1021/nn303539y

© 2012 American Chemical Society

pyrene-modified azobenzene was used for noncovalent functionalization of carbon nanotubes and graphene by  $\pi$ - $\pi$  interaction.<sup>21,22</sup> The mobility of graphene functionalized with azobenzene was 1700–2000  $\text{cm}^2/\text{V}\cdot\text{s}$ , which was very similar to the mobility of mechanically exfoliated graphene, 1800–2000  $\text{cm}^2/\text{V}\cdot\text{s}$ .<sup>22</sup> Besides, the chromophores on carbon nanotubes or graphene exhibited light-modulated responses in conduction and doping. However, due to the relatively slow kinetics of photoisomerization (from trans to cis) on graphene, the light response in conductance change was slow and the signal-to-noise ratio was very low.

Spiropyran (SP), which is a well-known photochromic molecule, has been used for molecular switches<sup>23</sup> and molecular sensors.<sup>24</sup> SP is changed to charge-separated merocyanine (MC) of purple color upon UV light exposure and returns back to colorless neutral SP upon visible light exposure or dark condition. The structural difference between SP and MC induces a difference in electrical and optical properties which are reversibly controlled upon alternating UV and visible light irradiation.<sup>25–27</sup> To date, SP has been used for functionalization of single-walled carbon nanotubes (CNTs) by both covalent and noncovalent bonding methods.<sup>28–31</sup> Due to the appearance and disappearance of the absorption band at 590 nm upon UV and visible light irradiation, respectively, it has potential for optical switching devices.<sup>30</sup> In addition, the electrical property of a CNT could also be tuned by functionalization of the CNT with pyrene-modified SP.<sup>31</sup> The threshold voltage of a CNT-based FET device was shifted to the direction of negative gate voltage because of a net negative charge transfer from pyrene-modified SP to CNT, and the conductance of CNTs functionalized with SP reversibly changed upon UV and visible light irradiation. Basically, the functionalization of graphene with a photochromic molecule by noncovalent bonding has many advantages, such as the defect-free doping effect and the possibility to control the graphene doping level using light exposure without defect generation.

Herein, we show the defect-free n-doping of graphene and its reversible modulation of the Dirac point and mobility by functionalization with SP *via* noncovalent bonding. The functionalization of graphene was successfully carried out by using pyrene-modified SP. Pyrene is well-adsorbed on graphene by  $\pi$ - $\pi$  interaction. This study describes optoelectronic properties of graphene which are reversibly modulated by conversion between SP and MC upon alternating UV and visible light irradiation.

## RESULTS AND DISCUSSION

Functionalization of graphene by noncovalent bonding was tried with the pyrene-modified spiropyran (SP) molecule which was synthesized by a known method.<sup>32</sup> (Figure S1 in the Supporting Information

shows a schematic diagram of the pyrene-modified spiropyran.) The photochromic SP moiety is connected to graphene through the pyrene moiety, which is attached on the graphene surface *via*  $\pi$ - $\pi$  interaction. This study investigates how the electrical property of graphene in a field-effect transistor is affected by the photochromic SP moiety on UV and visible light irradiation. Actually, the colorless SP in a solution is changed to the purple MC upon UV light irradiation, which is proved by the appearance of an absorption band at 560 nm (see Figure S2). In addition to such color change with UV irradiation, it is an interesting thing that a dipole field is generated by the MC because the neutral SP form has a closed ring structure but the MC form has an open structure with separated charges.<sup>25–27</sup> The MC form returns back to the SP form upon visible light irradiation or in darkness.

We fabricated a field-effect transistor device with single-layer graphene. Graphene was grown on Cu foil by the chemical vapor deposition (CVD) method and then was transferred onto a 300 nm  $\text{SiO}_2/\text{Si}$  wafer using a common transfer method.<sup>4</sup> The graphene FET device was immersed into a solution with pyrene-modified SP for 24 h, followed by rinsing with acetone to remove any unbound SP and then drying with  $\text{N}_2$ . It is well-known that the pyrene is adsorbed on graphene through  $\pi$ - $\pi$  interaction. Figure 1 shows a simple scheme of a FET device with graphene functionalized with SP and photoconversion from SP to MC.

Figure 2 shows the Raman spectra of pristine graphene, graphene functionalized with SP (SP-graphene), and SP-graphene after UV and visible light irradiation. It is confirmed that pristine graphene has just a little defect because its Raman spectrum shows the D band with very small intensity. Pyrene-modified SP is functionalized to graphene by noncovalent bonding, so it does not generate any change in the crystal structure of graphene. So, a defect was not generated in the graphene. Note that a small increase of D band intensity in the Raman spectrum of SP-graphene is due to an overall increase of all bands including G and 2D bands. Even though we now do not understand the reason for the increase of the Raman signal for SP-graphene, we assume that the increase of the Raman signal is due to resonant enhancement by similarity of the chemical structures between pyrene-modified SP and graphene.<sup>33</sup> It is interesting that the baseline of the SP-graphene Raman spectrum rose and became broad after UV irradiation, which is due to the fluorescence of MC converted from SP by UV irradiation.<sup>34</sup> Also, the UV irradiation induced appearance of many bands between 1100 and 1500  $\text{cm}^{-1}$  which is due to the resonance effect.<sup>35</sup> The resonance effect in the MC form is expected because it shows absorption at 560 nm (Figure S2). On the other hand, the Raman baseline was suppressed after sequential visible light irradiation, and after visible light irradiation for 30 min, it finally

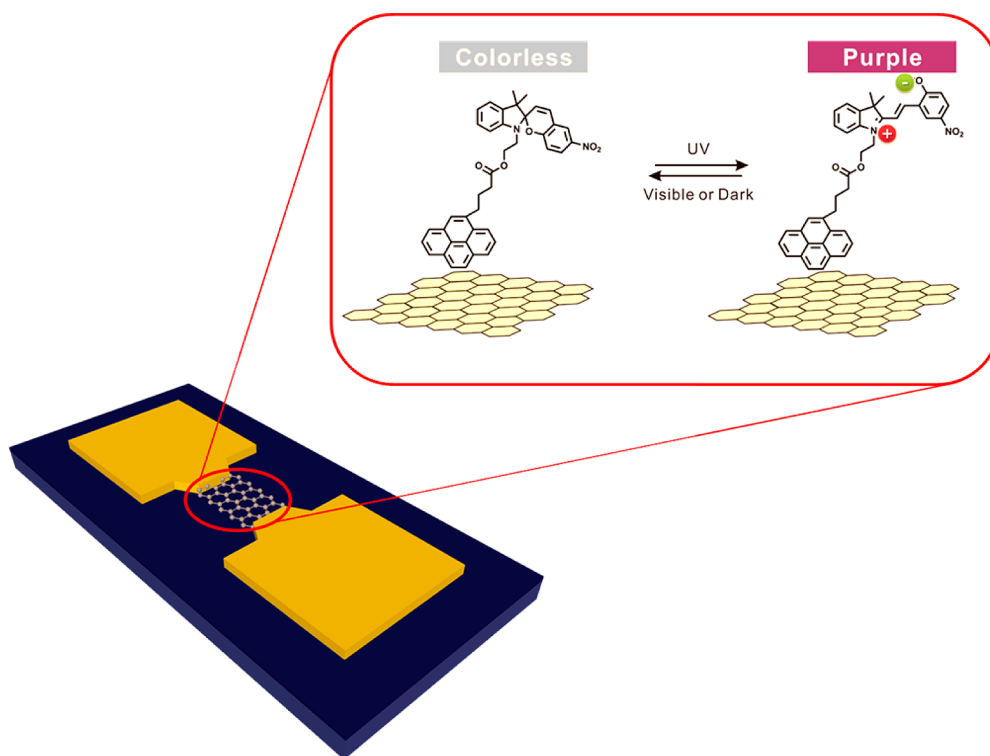


Figure 1. Schematic of a FET device with graphene functionalized with spiropyran.

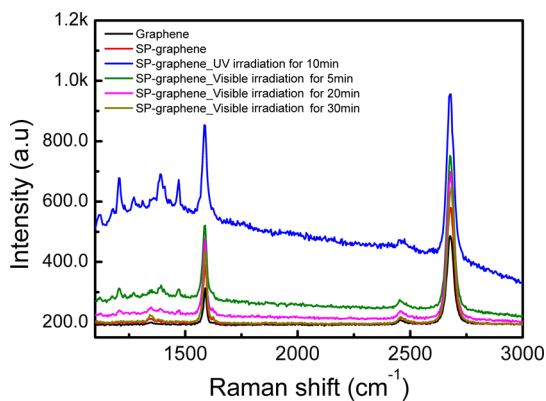


Figure 2. Raman spectra of pristine graphene, graphene functionalized with spiropyran (SP-graphene), and graphene functionalized with spiropyran after UV and visible irradiation.

became same as that of SP-graphene before UV irradiation. The Raman bands between 1100 and 1500  $\text{cm}^{-1}$  also disappeared after visible light irradiation for 30 min. The above changes in Raman spectra were reversible by alternating UV and visible irradiation. Note that the Raman spectrum of SP-graphene after UV light irradiation was not affected by 532 nm laser as an excitation wavelength for gathering the Raman signal because the exposure time of the 532 nm laser was very short, 1 s. As a control experiment, pyrene-coated graphene did not show any resonance Raman effect at an excitation wavelength of 532 nm.

Figure 3 shows the drain current ( $I_D$ ) as a function of the gate voltage ( $V_g$ ) of pristine graphene and

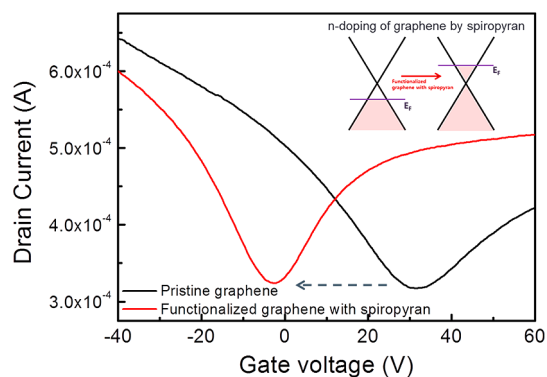
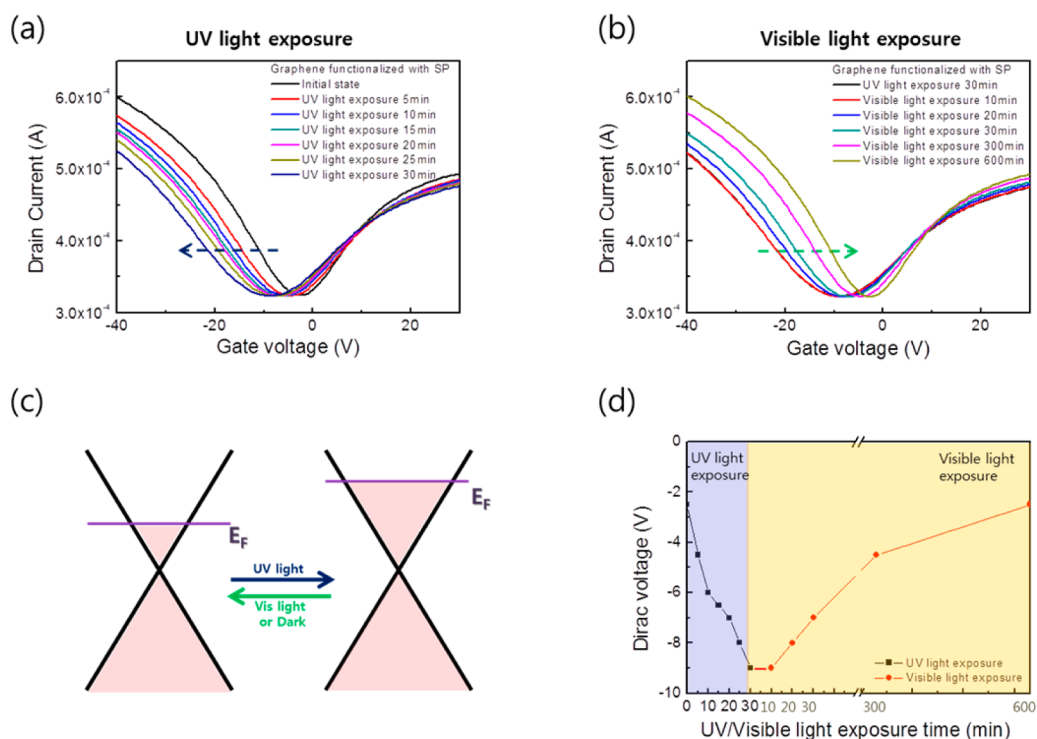


Figure 3.  $I$ – $V_g$  curves for the FET device with graphene before (black curve) and after (red curve) functionalization with spiropyran.

graphene functionalized with SP. The Dirac point of the pristine graphene device was 31.5 V, and charge carrier mobility was calculated to be 338.6 and 234.0  $\text{cm}^2/\text{V}\cdot\text{s}$  for hole and electron, respectively. The mobility was calculated by using the following equation,  $\mu_{FE} = g_m L / V_D W C_g$ ;  $g_m$  is transconductance,  $V_D$  is source–drain voltage,  $L$  is length,  $W$  is width, and  $C_g$  is capacitance of 300 nm  $\text{SiO}_2$ . The p-type behavior of a pristine graphene FET is usually caused by adsorbed oxygen or water. When graphene was functionalized with SP, the Dirac point was shifted from 31.5 V to  $-2.5$  V, indicating an n-doping effect. The n-doping of graphene is considered to be due to net negative charge transferred from the functionalized SP to graphene and due to cleaning the surface of the graphene by adsorption of pyrene-modified SP.<sup>31</sup> So the



**Figure 4.** (a) Dirac point change in  $I-V_g$  curves for FET with graphene functionalized with SP upon UV light exposure, and (b) Dirac point change in  $I-V_g$  curves for FET with graphene functionalized with SP upon visible light exposure. (c) Energy level change upon UV and visible light exposure. (d) Dirac point change as a functional of UV and visible light exposure time.

Fermi energy in graphene is changed, as displayed by the scheme in the inset of Figure 3. The charge carrier mobility slightly increased from 338.6 to 508.8  $\text{cm}^2/\text{V}\cdot\text{s}$  for hole and 234.0 to 428.4  $\text{cm}^2/\text{V}\cdot\text{s}$  for electron. The increase in charge carrier mobility may be because the functionalization with pyrene-modified SP makes the graphene surface clean by removing adsorbates. It also indicates that the functionalization with pyrene-modified SP did not induce any defect in graphene because it occurred by noncovalent bonding  $\pi-\pi$  interaction.

Many researchers have studied the doping of graphene to control its electrical properties and to tune its energy level for electronic device applications. So far, most of these studies have focused on the substitutional doping of graphene by an annealing process with  $\text{N}_2$  or  $\text{NH}_3$  gas.<sup>14</sup> However, inevitable defects were generated by these doping methods, and thus the carrier mobility in graphene decreased dramatically, by over 60%.<sup>14</sup> The simple deposition of metals such as Au, Ti, Fe, and K on the graphene surface has also been used for graphene doping.<sup>36,37</sup> The drawbacks in these kinds of doping call for a new approach such as the functionalization of graphene *via* noncovalent bonding. Very recently, the doping of graphene using noncovalent bonding was introduced. Kim *et al.* reported the p-doping of mechanically exfoliated graphene with pyrene-modified azobenzene without decrease of mobility.<sup>22</sup>

Since the structural change of photochromic molecules between SP and MC is reversible upon alternating UV and visible light irradiation, it is expected that it

would be possible to tune the position of the Fermi level (Dirac point in  $I-V_g$  curve). Actually, we could observe the reversible and repeatable change of the Dirac point in  $I-V_g$  curves upon UV and visible light exposure, as shown in Figure 4. In Figure 4a,b,  $I-V_g$  curves were measured with increasing time under UV (a) and visible (b) light irradiation. A portable hand-held ultraviolet lamp (365 nm, 4 W) and 150 W halogen incandescent lamp were used for UV and visible light irradiation, respectively. Note that the Dirac point of the pristine graphene was not changed upon UV light irradiation (Figure S3). On the other hand, graphene functionalized with SP showed a change of the Dirac point with UV light irradiation, which induced the conformational change of SP to MC on graphene. In Figure 4a, the Dirac point of the SP-functionalized graphene shifted from  $-2.5$  to  $-9$  V after UV light irradiation for 30 min, indicating further n-doped graphene (Figure 4c). In addition, the hole and electron mobility of the functionalized graphene slightly decreased to 392.4 from 508.8  $\text{cm}^2/\text{V}\cdot\text{s}$  and to 301.2 from 428.4  $\text{cm}^2/\text{V}\cdot\text{s}$ , respectively, after UV light exposure for 30 min. It is assumed that the mobility is slightly decreased because the charge-separated MC state is a scattering site. Upon visible light irradiation, the Dirac point returned back to the initial value,  $-2.5$  V (Figure 4b). The mobility increased to the initial values, as well. This means that changes in Dirac point and mobility are reversible upon alternating UV and visible light irradiation, and the doping level of graphene functionalized with SP can be controlled. Charge-separated MC lowers

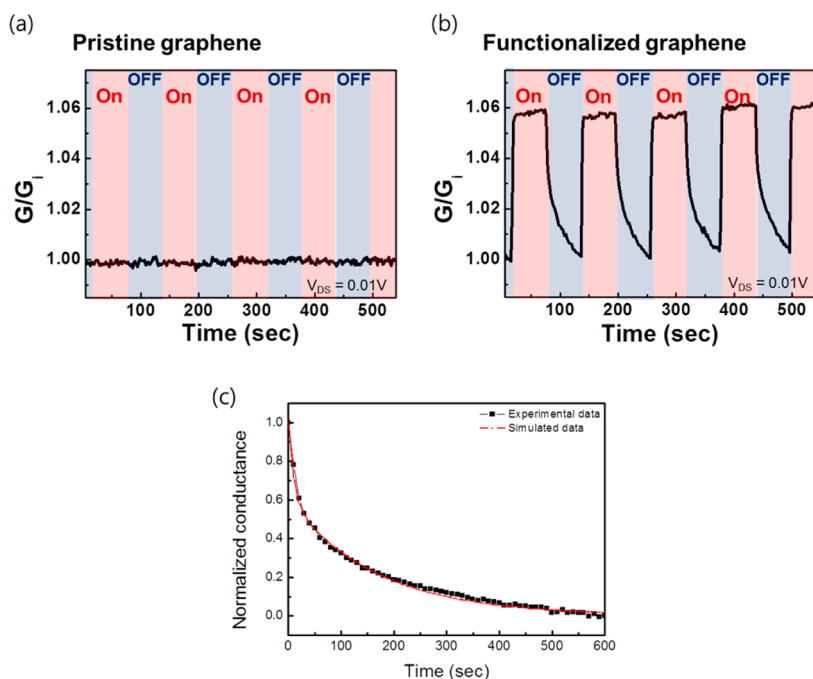


**Figure 5.** Conductance change in FET devices (a) with pristine graphene and (b) with graphene functionalized with spiropyran in vacuum. The bias between the source and drain electrodes is 10 mV, and the gate bias is 0 V.  $G$  is conductance and  $G_i$  is initial conductance. (c) Biexponential fitting result of conductance at 0 V gate bias vs time under darkness.

the Fermi level, while SP raises it (Figure 4c). Note that it took a longer time for the Dirac point to return to the initial value upon visible light irradiation (Figure 4d).

The reversible changes of Dirac point and mobility in FETs with functionalized graphene is due to the reversible conformational change between SP and MC on graphene upon UV and visible light irradiation. However, it remains unclear just how such a conformational change between SP and MC affects the Dirac point and mobility of graphene. This is a topic of future study. One possibility which we propose here is that the effect may be due to the charge separation in the MC created by UV light exposure. The charges in the MC form generate a localized dipole field on graphene which may affect the shift in the Dirac point.<sup>31</sup> Actually, this is similar to the results in a single-layer graphene FET with dual gates, where an electric field created by back-gate bias affected the position of the Dirac point of a top-gated graphene FET device.<sup>2</sup> The charge-separated MC can also play a role as a scattering site for the carriers. This site scatters carriers, inducing the decrease in mobility.

Figure 5 shows changes in the conductance of pristine graphene and functionalized graphene upon UV light on and off. As a control experiment, no conduction change was observed in the pristine graphene device (Figure 5a). On the other hand, the conductance change of the functionalized graphene device was pronounced, and the conductance increased by 6% upon UV light irradiation. Compared to the conductance change on graphene functionalized with azobenzene,<sup>22</sup> Figure 5b shows a high signal-to-noise ratio and very fast response. It is assumed that the

conformational change between cis and trans in azobenzene on graphene is slow, whereas that between SP and MC on graphene is fast. Actually, the decay time constant ( $\tau$ ) of trans to cis conversion in azobenzene on graphene was 302 s.<sup>22</sup> In Figure 5b, the conductance of graphene increased during the generation of the dipole field by the conversion from SP to MC upon UV light exposure but decreased during the extinction of the dipole field by the conversion from MC to SP in darkness. The conversion process of MC to SP under dark condition can be described by a biexponential expression,  $G = G_0[x \exp(-k_1 t) + (1 - x) \exp(-k_2 t)]$ .<sup>38</sup> The biexponential fitting indicates that two types of MCs= with decay rates  $k_1$  and  $k_2$  exist, and their fractions are  $x$  and  $1 - x$ . Details of the two types of MC are now unclear. We assume that one is a separated MC on graphene and the other is a stack of MC (aggregates of MC) on graphene. Another interesting point is the kinetics of MC conversion to SP on graphene because such conversion may show different behaviors in the cases of free SP in solution, SP grafted to polymer, and SP adsorbed on graphene *via* pyrene. With the biexponential fitting in Figure 5c, the half-life ( $\tau$ ) of MC conversion to SP on the graphene was calculated to be 34.6 s. The half-life of the conversion on graphene is much shorter compared to that in cases of other solid-state samples, such as SP-grafted polymers and SP on gold nanoparticle, and even is comparable to that in solutions with SP-grafted polymers. For reference, the half-life of the conversion was between 9.6 and 497 s in solutions with SP-grafted polymers and was over 74.6 min in solid samples of SP-grafted polymers.<sup>38</sup>

The half-life of the conversion in SP-modified gold nanoparticles was 23 min.<sup>39</sup>

## CONCLUSION

In summary, we have demonstrated defect-free n-doping of graphene by using functionalization with SP by noncovalent bonding. The conformational

change between SP and MC on UV and visible (or dark) light irradiation affected the electrical properties of graphene. We demonstrated a reversible light-modulated Dirac point of graphene according to UV and visible light exposure. This allows for new possibilities of doping control methods using functionalization of graphene with photochromic molecules.

## EXPERIMENTAL METHODS

**Synthesis of Graphene Using CVD.** Graphene was prepared by a common chemical vapor deposition (CVD) method. Copper foil (99.8% purity, 0.025 mm thick, Alfa Aesar) was positioned in a 2 in. quartz tube CVD system. It was heated to 1050 °C with 10 sccm hydrogen gas and subsequently 5 sccm CH<sub>4</sub> gas flow for 15 min. After that, the furnace was quickly cooled to room temperature. The front side of the graphene on the Cu foil was covered with PMMA, and the back side of the graphene on the Cu foil was removed with O<sub>2</sub> plasma (Femto, Diener). The graphene grown on the Cu foil was etched by 0.1 M ammonia persulfate (Sigma Aldrich), followed by wash with fresh DI water several times. Then, graphene was transferred to a Si substrate with 300 nm thermal oxide.

**Fabrication of Graphene FET Device and Functionalized with Pyrene-Modified Spiropyran.** Graphene channels patterned on a Si substrate with 300 nm thermal oxide were used for device fabrication by electron beam lithography (Nanobeam nB4, NBL), O<sub>2</sub> plasma, metal deposition (Ti (5 nm)/Au (35 nm)), and lift-off process. The channel of the graphene FET is 1 μm in length and 2 μm width. The fabricated graphene FET device was functionalized by dipping it into a solution with pyrene-modified spiropyran for 24 h. After that, it was rinsed with acetone to remove unbound molecules and dried in N<sub>2</sub>.

**Analysis of Graphene with Pyrene-Modified Spiropyran and Measurement of Graphene FET Devices.** Raman spectroscopy (WiTec) was used to check the quality of graphene after the transfer process. Raman spectra of SP-graphene after UV and visible irradiation were measured to check if the functionalization was successful and the conformational change occurred. The 532 nm laser as an excitation source was used, and the laser power was 2 mW, which avoids any damage or heating of the graphene during the measurement. Exposure time is 1 s, and the calibration was done using a reference Si peak position at 520 cm<sup>-1</sup>. The fabricated graphene FET device was loaded into a vacuum chamber (Lake Shore) for electrical measurement. Electrical properties of the FET device of pristine and functionalized graphene were characterized in vacuum (~10<sup>-5</sup> Torr) with a semiconductor parameter analyzer (4200-SCS semiconductor parameter analyzer, Keithley). Every electrical measurement was done in a vacuum condition near 10<sup>-5</sup> Torr, and thus we could measure only changes of electrical property of the graphene due to the SP without any effect by oxygen and water molecules in air.

**Conflict of Interest:** The authors declare no competing financial interest.

**Acknowledgment.** This work was supported by the WCU (World Class University) program (R31-2008-000-20012-0 and R31-2008-10029), the Basic Science Research Program (2011-0013601), and the grant (Code No. 2011-0031630 and 2011-0032153) from the Center for Advanced Soft Electronics under the Global Frontier Research Program through the National Research Foundation funded by MEST of Korea.

**Supporting Information Available:** Additional information for synthetic scheme of spiropyran, UV/vis absorption spectra upon UV irradiation, and  $I-V_g$  curves of pristine graphene upon UV light irradiation. This material is available free of charge via the Internet at <http://pubs.acs.org>.

## REFERENCES AND NOTES

- Novoselov, K. S.; Geim, A. K.; Morozov, S. V.; Jiang, D.; Zhang, Y.; Dubonos, S. V.; Grigorieva, I. V.; Firsov, A. A. Electric Field Effect in Atomically Thin Carbon Films. *Science* **2004**, *306*, 666–669.
- Avouris, P. Graphene: Electronic and Photonic Properties and Devices. *Nano Lett.* **2010**, *10*, 4285–4294.
- Kim, K. S.; Zhao, Y.; Jang, H.; Lee, S. Y.; Kim, J. M.; Kim, K. S.; Ahn, J.; Kim, P.; Choi, J.; Hong, B. H. Large-Scale Pattern Growth of Graphene Films for Stretchable Transparent Electrodes. *Nature* **2009**, *457*, 706–710.
- Li, X.; Cai, W.; An, J.; Kim, S.; Nah, J.; Yang, D.; Piner, R.; Velamakanni, A.; Jung, I.; Tutuc, E.; *et al.* Large-Area Synthesis of High-Quality and Uniform Graphene Films on Copper Foils. *Science* **2009**, *324*, 1312–1314.
- Bae, S.; Kim, H.; Lee, Y.; Xu, X.; Park, J.; Zheng, Y.; Balakrishnan, J.; Lei, T.; Kim, H. R.; Song, Y. I.; *et al.* Roll-to-Roll Production of 30-Inch Graphene Films for Transparent Electrodes. *Nat. Nanotechnol.* **2010**, *5*, 574–578.
- Novoselov, K. S.; Geim, A. K.; Morozov, S. V.; Jiang, D.; Katsnelson, M. I.; Grigorieva, I. V.; Dubonos, S. V.; Firsov, A. A. Two-Dimensional Gas of Massless Dirac Fermions in Graphene. *Nature* **2005**, *438*, 197–200.
- Zhang, Y.; Tan, Y.; Stormer, H. L.; Kim, P. Experimental Observation of the Quantum Hall Effect and Berry's Phase in Graphene. *Nature* **2005**, *438*, 201–204.
- Meric, I.; Han, M.; Young, A. F.; Ozyilmaz, B.; Kim, P.; Shepard, K. L. Current Saturation in Zero-Bandgap, Top-Tated Graphene Field-Effect Transistors. *Nat. Nanotechnol.* **2008**, *3*, 654–659.
- Castro, E. V.; Novoselov, K. S.; Morozov, S. V.; Peres, N. M. R.; Santos, J. M. B.; Nilsson, J.; Guinea, F.; Geim, A. K.; Castro Neto, A. H. Biased Bilayer Graphene: Semiconductor with a Gap Tunable by the Electric Field Effect. *Phys. Rev. Lett.* **2007**, *99*, 216802.
- Xia, F.; Farmer, D. B.; Lin, Y.; Avouris, P. Graphene Field-Effect Transistors with High On/Off Current Ratio and Large Transport Band Gap at Room Temperature. *Nano Lett.* **2010**, *10*, 715–718.
- Li, X.; Wang, X.; Zhang, L.; Lee, S.; Dai, H. Chemically Derived, Ultrasoft Graphene Nanoribbon Semiconductors. *Science* **2008**, *319*, 1229–1232.
- Bai, J.; Zhong, X.; Jiang, S.; Huang, Y.; Duan, X. Graphene Nanomesh. *Nat. Nanotechnol.* **2010**, *5*, 190–194.
- Chen, J. H.; Jang, C.; Adam, S.; Fuhrer, M. S.; Williams, E. D.; Ishigami, M. Charged-Impurity Scattering in Graphene. *Nat. Phys.* **2008**, *4*, 377–381.
- Guo, B.; Liu, Q.; Chen, E.; Zhu, H.; Fang, L.; Gong, J. R. Controllable N-Doping of Graphene. *Nano Lett.* **2010**, *10*, 4975–4980.
- Wang, X.; Li, X.; Zhang, L.; Yoon, Y.; Weber, P. K.; Wang, H.; Guo, J.; Dai, H. N-Doping of Graphene through Electrothermal Reactions with Ammonia. *Science* **2009**, *324*, 768–771.
- Wei, D.; Liu, Y.; Wang, Y.; Zhang, H.; Huang, L.; Yu, G. Synthesis of N-Doped Graphene by Chemical Vapor Deposition and Its Electrical Properties. *Nano Lett.* **2009**, *9*, 1752–1758.
- Sun, Z.; Yan, Z.; Yao, J.; Beitler, E.; Zhu, Y.; Tour, J. M. Growth of Graphene from Solid Carbon Sources. *Nature* **2010**, *468*, 549–552.

18. Bekyarova, E.; Itkis, M. E.; Ramesh, P.; Berger, C.; Sprinkel, M.; Heer, W. A.; Haddon, R. C. Chemical Modification of Epitaxial Graphene: Spontaneous Grafting of Aryl Groups. *J. Am. Chem. Soc.* **2009**, *131*, 1336–1337.
19. Huang, P.; Zhu, H.; Jing, L.; Zhao, Y.; Gao, X. Graphene Covalently Binding Aryl Groups: Conductivity Increases Rather than Decreases. *ACS Nano* **2011**, *5*, 7945–7949.
20. Sinitskii, A.; Dimiev, A.; Corley, D. A.; Fursina, A. A.; Kosynkin, D. V.; Tour, J. M. Kinetics of Diazonium Functionalization of Chemically Converted Graphene Nanoribbons. *ACS Nano* **2010**, *4*, 1949–1954.
21. Simmons, J. M.; In, I.; Campbell, V. E.; Mark, T. J.; Leonard, F.; Gopalan, P.; Eriksson, M. A. Optically Modulated Conduction in Chromophore-Functionalized Single-Wall Carbon Nanotubes. *Phys. Rev. Lett.* **2007**, *98*, 086802.
22. Kim, M.; Safron, N. S.; Huang, C.; Arnold, M. S.; Gopalan, P. Light-Driven Reversible Modulation of Doping in Graphene. *Nano Lett.* **2012**, *12*, 182–187.
23. Kocer, A.; Walko, M.; Meijberg, W.; Feringa, B. L. A Light-Actuated Nanovalve Derived from a Channel Protein. *Science* **2005**, *309*, 755–758.
24. Byrne, R.; Diamond, D. Chemo/Bio-Sensor Networks. *Nat. Mater.* **2006**, *5*, 421–424.
25. Krysanov, S. A.; Alfimov, M. V. Ultrafast Formation of Transients in Spiropyran Photochromism. *Chem. Phys. Lett.* **1982**, *91*, 77–80.
26. Berkovic, G.; Krongauz, V.; Weiss, V. Spiroyrans and Spirooxazines for Memories and Switches. *Chem. Rev.* **2000**, *100*, 1741–1753.
27. Sanchez-Lozano, M.; Estevez, C. M.; Hermida-Ramon, J.; Serrano-Andres, L. Ultrafast Ring-Opening/Closing and Deactivation Channels for a Model Spiropyran-Merocyanine System. *J. Phys. Chem. A* **2011**, *115*, 9128–9138.
28. Canto, E. D.; Flavin, K.; Natali, M.; Perova, T.; Giordani, S. Functionalization of Single-Walled Carbon Nanotubes with Optically Switchable Spiroyrans. *Carbon* **2010**, *48*, 2815–2824.
29. Khairutdinov, R. F.; Itkis, M. E.; Haddon, R. C. Light Modulation of Electronic Transitions in Semiconducting Single Wall Carbon Nanotubes. *Nano Lett.* **2004**, *4*, 1529–1533.
30. Setaro, A.; Bluemmel, P.; Maity, C.; Hecht, S.; Reich, S. Non-covalent Functionalization of Individual Nanotubes with Spiropyran-Based Molecular Switches. *Adv. Funct. Mater.* **2012**, *22*, 2425–2431.
31. Guo, X.; Huang, L.; O'Brien, S.; Kim, P.; Nuckolls, C. Directing and Sensing Changes in Molecular Conformation on Individual Carbon Nanotube Field Effect Transistors. *J. Am. Chem. Soc.* **2005**, *127*, 15045–15047.
32. Raymo, F. M.; Giordani, S. Signal Processing at the Molecular Level. *J. Am. Chem. Soc.* **2001**, *123*, 4651–4652.
33. Ling, X.; Xie, L.; Fang, Y.; Xu, H.; Zhang, H.; Kong, J.; Dresselhaus, M. S.; Zhang, J.; Liu, Z. Can Graphene Be Used as a Substrate for Raman Enhancement? *Nano Lett.* **2010**, *10*, 553–561.
34. Zhu, M.; Zhu, L.; Han, J. J.; Wu, W.; Jurst, J. K.; Li, A. D. Q. Spiropyran-Based Photochromic Polymer Nanoparticles with Optically Switchable Luminescence. *J. Am. Chem. Soc.* **2006**, *128*, 4303–4309.
35. Aramaki, S.; Atkinson, G. H. Spiroanthropyran Photochromism: Picosecond Time-Resolved Spectroscopy. *J. Am. Chem. Soc.* **1992**, *114*, 438–444.
36. Shi, Y.; Kim, K. K.; Reina, A.; Hofmann, M.; Li, L.; Kong, J. Work Function Engineering of Graphene Electrode via Chemical Doping. *ACS Nano* **2010**, *5*, 2689–2694.
37. Pi, K.; McCreary, K. M.; Bao, W.; Han, W.; Chiang, Y. F.; Li, Y.; Tsai, S.; Lau, C. N.; Kawakami, R. K. Electronic Doping and Scattering by Transition Metals on Graphene. *Phys. Rev. B* **2009**, *80*, 075406.
38. Allcock, H. R.; Kim, C. Photochromic Polyphosphazenes with Spiropyran Units. *Macromolecules* **1991**, *24*, 2846–2851.
39. Ipe, B. I.; Mahima, S.; Thomas, K. G. Light-Induced Modulation of Self-Assembly on Spiropyran-Capped Gold Nanoparticles: A Potential System for the Controlled Release of Amino Acid Derivatives. *J. Am. Chem. Soc.* **2003**, *125*, 7174–7175.